The simplest demonstrations of quantum nonlocality

2012 New J. Phys. 14 113020

(http://iopscience.iop.org/1367-2630/14/11/113020)

New Journal of Physics
The open access journal for physics

The simplest demonstrations of quantum nonlocality

Dylan J Saunders[1], Matthew S Palsson[1], Geoff J Pryde[1,3], Andrew J Scott[1], Stephen M Barnett[2,3] and Howard M Wiseman[1,3]

[1] Centre for Quantum Computation and Communication Technology (Australian Research Council), Centre for Quantum Dynamics, Griffith University, Brisbane 4111, Australia
[2] Department of Physics, University of Strathclyde, Glasgow G4 0NG, UK
E-mail: G.Pryde@griffith.edu.au, Steve@phys.strath.ac.uk and H.Wiseman@griffith.edu.au

New Journal of Physics **14** (2012) 113020 (12pp)
Received 6 July 2012
Published 15 November 2012
Online at http://www.njp.org/
doi:10.1088/1367-2630/14/11/113020

Abstract. We investigate the complexity cost of demonstrating the key types of nonclassical correlations—Bell inequality violation, Einstein, Podolsky, Rosen (EPR)-steering, and entanglement—with independent agents, theoretically and in a photonic experiment. We show that the complexity cost exhibits a hierarchy among these three tasks, mirroring the recently discovered hierarchy for how robust they are to noise. For Bell inequality violations, the simplest test is the well-known Clauser–Horne–Shimony–Holt test, but for EPR-steering and entanglement the tests that involve the fewest number of detection patterns require nonprojective measurements. The simplest EPR-steering test requires a choice of projective measurement for one agent and a single nonprojective measurement for the other, while the simplest entanglement test uses just a single nonprojective measurement for each agent. In both of these cases, we derive our inequalities using the concept of circular two-designs. This leads to the interesting feature that in our photonic demonstrations, the correlation of interest is independent of the angle between the linear polarizers used by the two parties, which thus require no alignment.

[3] Authors to whom any correspondence should be addressed.

Contents

1. Introduction 2
2. Defining the problem 3
3. Positive operator valued measures, spherical designs and the singlet correlations 5
4. Quantum nonlocality tests 7
5. Experiment 8
6. Conclusion 11
Acknowledgments 11
Appendix. Measurement efficiency 11
References 12

1. Introduction

Nonclassical correlations are a powerful resource for information processing, and studying them opens a window on the true nature of the quantum world. For example, entanglement appears to be a requirement for universal quantum computing, while violations of Bell inequalities reveal that it is not possible to describe certain physical phenomena using any local realistic model [1].

Recently there has been significant interest in the hierarchy of nonclassical correlations. It has been known for some time that not all entangled states are capable of violating a Bell inequality [2]. In 2007, the Einstein–Podolsky–Rosen (EPR)-steering phenomenon was added to this ladder of effects. EPR-steering is a formalization [3, 4] of Einstein's 'spooky action at a distance'— the EPR effect [5, 6]— called 'steering' by Schrödinger [7]. This formalization was achieved by turning EPR-steering into a real-world quantum information *task*, in which mixed states and arbitrary (nonprojective) measurements must be considered [3, 4]. Schrödinger's term is appropriate because this task can be performed only if one party (Alice) demonstrates that she can steer the state of the other party's (Bob's) sub-system, via her choice of measurement setting. That is, EPR-steering is demonstrated if and only if Bob is forced to admit that he cannot describe his system by a local quantum state unaffected by Alice's actions. Note that while Bob's measurement apparatus is assumed trustworthy, just as in entanglement tests, no assumptions are made about the apparatus that generates Alice's declared outcomes, just as in Bell tests.

Every Bell inequality violation is an EPR-steering demonstration (but not vice versa) and every EPR-steering demonstration witnesses entanglement (but not vice versa). Thus these three concepts form a logical hierarchy. Moreover, this logical hierarchy gives rise to a *strict* hierarchy of states that can be used to demonstrate these nonlocal phenomena: the set of states that can be used to demonstrate Bell-nonlocality is a strict subset of those that can manifest EPR-steering, which is likewise a strict subset of those showing entanglement [3, 4]. Recently this strict hierarchy has been demonstrated experimentally using a range of two-qubit Werner states, and utilizing projective measurements [8]. It has also been extended theoretically to higher dimensional spin systems [9]. The strict hierarchy of nonclassical correlations also extends to the quantum information protocols they enable. For example, a Bell inequality violation can provide device-independent security for quantum key distribution—Alice and Bob can be certain to share a secure key, even if each of their apparatus was provided by an

eavesdropper [10]. EPR-steering inequalities, on the other hand, enable an asymmetric form of this security in which only Bob's detector need be trusted [11]. In both cases, closing the detection loophole is essential, and this was recently demonstrated for EPR-steering in a number of photonic experiments [12–14].

One might be tempted to conclude that strict hierarchies like the above will always exist. That is not the case, however. As shown theoretically and experimentally in [12], in the absence of mixture, there is no strict hierarchy for loss tolerance, in the sense that EPR-steering *with no detection loophole* can be demonstrated with arbitrarily low detector efficiency for Alice as well as Bob, just as for entanglement witnessing. Another case in which the hierarchy is not strict is the communication cost for colluding parties to simulate nonlocality. The number of bits of classical communication required to simulate correlations demonstrating entanglement and steering is zero, but for correlations demonstrating Bell nonlocality it is nonzero [15, 16].

It is thus nontrivial to discover a new context in which a strict hierarchy of Bell nonlocality, EPR-steering and entanglement exists. This paper reports precisely such a discovery, and its experimental verification. We do this not by asking what degree of purity of the state is required, nor what tasks are enabled, but rather: how complex an experiment is required? As well as establishing a hierarchy of complexity cost, this may have practical application in maximizing the bandwidth in quantum information protocols, such as entanglement distribution, that require nonlocal correlations.

To address this problem, we define the fundamental complexity 'cost' by the integer W, the number of different types of detection patterns (joint detection outcomes) that must occur. It is not *a priori* obvious that this will give a *strict* hierarchy but we find that it does: the most parsimonious (least complex) demonstrations of entanglement, EPR-steering, and Bell nonlocality require $W = 9$, 12, and 16 respectively. While the most parsimonious test of Bell nonlocality is the standard Clauser–Horne–Shimony–Holt (CHSH) [17] test using projective measurements, those for entanglement and EPR-steering both require generalized (nonprojective) measurements [18]. We implement these maximally parsimonious demonstrations experimentally using polarization-entangled photons. The demonstrations of entanglement and EPR-steering have the interesting feature that they do not require alignment of the polarizers between the parties: the degree of violation of the corresponding inequalities is independent of the relative angle.

This paper is structured as follows. In section 2 we define the problem precisely and show from very general principles that the costs for demonstrating entanglement, EPR-steering and Bell nonlocality cannot be lower than $W = 9$, 12, and 16 respectively. In section 3, we introduce a formalism, using the concept of one-designs and two-designs, to describe certain sorts of measurements on an entangled pair of qubits. This allows us, in section 4, to construct new nonlocality tests that prove that the above minimum W values for entanglement tests and EPR-steering can be attained. Finally (section 5), using photonic singlet states, we demonstrate experimentally the violation of these new inequalities using 'trine' measurements [18, 19], as well as a demonstration of the standard CHSH inequality.

2. Defining the problem

Consider an experimental demonstration of some particular type of quantum nonlocality involving $P \geqslant 2$ distinct parties. Let $S_p \geqslant 1$ be the number of different measurement settings used by party p, and $O_p^s \geqslant 2$ the number of possible outcomes of setting s for party p. Then the

definition of the complexity cost is

$$W = \prod_{p=1}^{P} \sum_{s=1}^{S_p} O_p^s. \tag{1}$$

In words, W is the number of possible patterns of joint detection outcomes that can occur. In the remainder of this paper, we restrict to $P = 2$, and name the two parties Alice and Bob. For $P > 2$ the minimum complexity cost is certainly never smaller than for $P = 2$, but we note that it is an interesting open question to consider the minimum W required to demonstrate 'genuine multipartite quantum nonlocality' (see e.g. [20]) of various kinds.

Note that we have taken the choice of setting each party to be independent. Dropping this assumption allows more parsimonious tests than those we consider, but at the cost of lowering security. Both entanglement and EPR-steering could be demonstrated by Alice and Bob with qubits and projective measurements, with only eight possible patterns: they can measure the correlation $\langle \hat{\sigma}_x \otimes \hat{\sigma}_x + \hat{\sigma}_z \otimes \hat{\sigma}_z \rangle$ if either both measure $\hat{\sigma}_x$, or both measure $\hat{\sigma}_z$. In the absence of communication between the parties, this would require Alice and Bob to have predetermined which of $\hat{\sigma}_x$ or $\hat{\sigma}_z$ they measure in each run. As stated, however, such predetermination opens a loophole in the tests, as we now explain for the two cases. For the case of EPR-steering, a rigorous test means that Alice is not trusted by Bob [3]. Clearly if Bob's settings are predetermined then Alice could trivially create a perfect correlation by sending Bob either $\hat{\sigma}_x$ eigenstates or $\hat{\sigma}_z$ eigenstates, as appropriate. For the simpler case of demonstrating entanglement both parties are considered trustworthy [3]. However, if the device supposedly creating the entanglement is untrusted—it might be supplied by a competitor, Eve—then the device could spy on the predetermined lists of settings and again create perfect correlations while generating only product states. For this reason we stick to the rigorous conditions in which the parties' choices are independent, giving equation (1).

We first show that the values of $W = 16$, 12 and 9 are the minimum possible to demonstrate Bell nonlocality, EPR-steering and entanglement, respectively. To demonstrate Bell nonlocality it is necessary for both Alice and Bob to have measurement choices; without this it is trivial to construct a local-hidden-variable model that explains the measurement outcomes. Thus the most parsimonious inequality is that found originally by Bell, and refined by CHSH [17], in which each party has two settings, and each setting has two outcomes. The Bell-nonlocality case therefore has $W_{\mathrm{B}} = 16$. Next, for EPR-steering it is again crucial for Alice to have a measurement choice (the task is for her to steer Bob's state by her choice of measurement), but Bob need not use more than one setting. However, if he uses only one setting then he cannot use a two-outcome measurement because the two positive operators corresponding to the two outcomes would necessarily commute, and hence be co-diagonal in some basis. Completely decohering Bob's system in that same basis would have no effect on his outcomes, but would of course completely destroy any entanglement with Alice's system and hence any possibility of demonstrating EPR-steering. Thus the smallest cost W in this case is when Alice has two settings with two outcomes each, and Bob has one setting with three outcomes, giving $W_{\mathrm{S}} = 12$. Finally, for demonstrating entanglement no choice is required on either side, but with this strategy it is necessary to have three-outcome measurements on both sides, using the same commutation argument, yielding a minimum of $W_{\mathrm{E}} = 9$. We also note that the hierarchy is preserved with respect to the number of measurement *settings*, i.e. the number of distinct configurations of the measurement apparatus. Demonstrations of the CHSH, EPR-steering and entanglement phenomena require 4, 2 and 1 measurement settings, respectively.

3. Positive operator valued measures, spherical designs and the singlet correlations

Consider an arbitrary N-outcome qubit POVM (positive operator valued measure; also called a POM [18]), $\{\hat{F}_k\}_{k=1}^N$ which is *sharp* [21, 22]. In other words, each $\hat{F}_k$ is proportional to a rank-one projector on the qubit Hilbert space. Each POVM element $\hat{F}_k$ can thus be defined by a unit-length three-vector $\vec{A}_k$, and a positive weight a_k by

$$\hat{F}_k = a_k(\hat{1} + \vec{A}_k \cdot \vec{\sigma}). \tag{2}$$

Here $\hat{1}$ is the qubit identity operator and $\vec{\sigma} = (\hat{\sigma}_x, \hat{\sigma}_y, \hat{\sigma}_z)^\top$ is the vector of Pauli operators. The POVMs have the completeness condition that $\sum_{k=1}^N \hat{F}_k = \hat{1}$, which implies that

$$\sum_{k=1}^N a_k = 1, \quad \sum_{k=1}^N a_k \vec{A}_k = \vec{0}. \tag{3}$$

Equation (3) is equivalent to the mathematical statement that the set $\mathbb{A} = \{a_k, \vec{A}_k\}_{k=1}^N$ forms a spherical one-design [27]. A spherical one-design is the simplest case of the class of spherical t-designs, defined for all $t \in \mathbb{N}$. Intuitively, as t increases this means that $\mathbb{A}$ is a better and better approximation to the set $\mathbb{S}$ of all unit vectors on the sphere S^2, distributed according to the $SO(3)$-Haar measure. Technically, a spherical t-design is such that all moments of order t (obtained by averaging over the set using the weights a_k) equal the corresponding moments of the set $\mathbb{S}$. The concept of t-designs has been extensively used in quantum information theory in recent years [23–26]. In this paper we are interested only in one-designs and two-designs.

Taking the above to apply to Alice's qubit, we likewise define POVM elements for Bob by $\hat{E}_j = b_j(\hat{1} + \vec{B}_j \cdot \vec{\sigma})$, with the analogous constraints on his set $\mathbb{B} = \{b_j, \vec{B}_j\}_{j=1}^M$. We will use $\mathbb{A}$ and $\mathbb{B}$ to denote Alice's and Bob's measurement.

Say Alice and Bob share the two-qubit singlet state

$$\rho_{\text{singlet}} = (1/4)(\hat{1} \otimes \hat{1} - \hat{\sigma}_x \otimes \hat{\sigma}_x - \hat{\sigma}_y \otimes \hat{\sigma}_y - \hat{\sigma}_z \otimes \hat{\sigma}_z).$$

From the Pauli algebra it is easy to verify that the probability for the joint outcome (k, j) is

$$P_{kj} = \text{Tr}[\rho_{\text{singlet}}(\hat{F}_k \otimes \hat{E}_j)] = a_k b_j (1 - \vec{A}_k \cdot \vec{B}_j). \tag{4}$$

Note that we are using Tr to denote a trace over a quantum Hilbert space; we reserve tr to denote a trace over a tensor relating to three-dimensional space (see below).

We wish to consider correlations between Alice's and Bob's outcomes. So far we have only labels k and j for these outcomes, but no physical reason for looking at any particular relation between them. We could look at the entire (discrete) probability distribution P_{kj}, as is done in exhaustive searches for Bell-inequality violations [28]. This is appropriate for investigating Bell-nonlocality, a concept that makes no reference to quantum mechanical properties of the systems. Here, however, we are interested in demonstrating other sorts of nonlocality in which such properties do play a role, namely entanglement and EPR-steering. Thus we seek a natural correlation function which uses the quantum physics of the problem. Rather than considering the outcome of Alice's measurement $\mathbb{A}$ to be the label k, we will consider it to be a unit vector $\vec{A}$, taking values $\vec{A}_k$ corresponding to the POVM elements $\hat{F}_k$, and likewise for Bob. Then

considering equation (4), the natural way to combine the two vector-valued random variables $\vec{A}$ and $\vec{B}$ is to construct the correlation function

$$\langle \vec{A} \cdot \vec{B} \rangle = \sum_{jk} P_{kj} \vec{A}_k \cdot \vec{B}_j. \tag{5}$$

Using the fact that $\mathbb{A}$ and $\mathbb{B}$ are spherical one-designs, and the singlet correlations (equation (4)), we find that the ensemble average (5) evaluates to the simple expression

$$\langle \vec{A} \cdot \vec{B} \rangle = -\mathrm{tr}\,[\mathbf{AB}]\,, \tag{6}$$

where we have defined the 3×3 tensor

$$\mathbf{A} = \sum_{k=1}^{N} a_k \vec{A}_k \vec{A}_k^{\top}, \tag{7}$$

and similarly for $\mathbf{B}$. Note that $\mathrm{tr}\,\mathbf{A} = \mathrm{tr}\,\mathbf{B} = 1$ from normalization.

Now if, in addition to equation (3), $\mathbb{A}$ has the property that $\mathbf{A} = (1/3)\mathbf{I}_3$, where $\mathbf{I}_3$ is the 3×3 identity tensor, then $\mathbb{A}$ forms a weighted spherical two-design on S^2 [29]. The simplest example of a spherical two-design on the two-sphere involves four equally weighted vectors $\vec{A}_j$ pointing to the vertices of a regular terahedron.

Say that $\mathbf{B} = (1/3)\mathbf{I}_3$, so that $\mathbb{B}$ is a weighted two-design on the sphere. Then for any one-design (that is, any measurement) $\mathbb{A}$, it follows from equation (6) that

$$\langle \vec{A} \cdot \vec{B} \rangle = -\mathrm{tr}\,\mathbf{A}/3 = -1/3. \tag{8}$$

That is, the correlation between Alice's and Bob's measurement results is *independent* of the weightings and three-dimensional orientation of the vectors that define their POVMs. This supports the idea that $\langle \vec{A} \cdot \vec{B} \rangle$ is a natural correlation function for qubit POVMs.

To derive the most parsimonious tests of EPR-steering and entanglement we actually wish to consider not spherical two-designs, but circular two-designs [29]. This applies if we restrict the $\vec{A}_k$ and $\vec{B}_j$ to lying in a single plane in the Bloch sphere (say the $y = 0$ plane). Then $\mathbb{B}$ being a circular two-design means $\sum_{j=1}^{M} b_j \vec{B}_j \vec{B}_j^{\top} = (1/2)\mathbf{I}_2$ where $\mathbf{I}_2$ is the 2×2 identity tensor (in the x–z plane). The simplest example of a circular two-design involves three equally weighted vectors $\vec{B}_j$ pointing to the vertices of an equilateral triangle in the x–z plane (see figure 1). The corresponding measurement is known as a trine measurement [18, 19]. For any circular two-design measurement by Bob, in which the $\vec{A}_k$ are restricted to the same plane, equation (8) is replaced by

$$\langle \vec{A} \cdot \vec{B} \rangle = -\mathrm{tr}\,\mathbf{A}/2 = -1/2. \tag{9}$$

It is still the case that the singlet correlation between Alice's and Bob's measurement results is independent of the weightings and planar arrangement of the vectors, only now the degree of correlation is higher.

From the discussions in section 2 we know that the simplest possible tests of entanglement or EPR-steering would involve two- or three-outcome measurements. Henceforth we now restrict, for simplicity, to the case where Bob makes a trine measurement, and Alice either a trine measurement or two orthogonal projective measurements. Both sides' measurements are assumed to lie in the same plane (e.g. linear polarization measurements) but we make no assumptions about the relative angle between Alice's and Bob's designs.

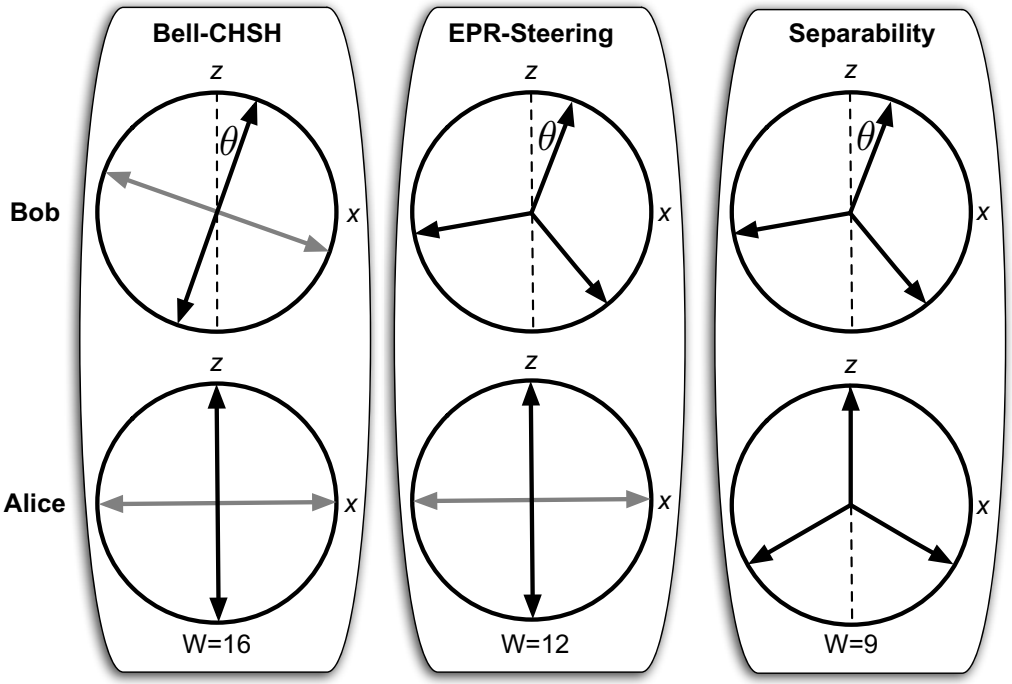

Figure 1. Measurement directions. The circle represents the x–z plane of the Bloch sphere, the dashed line shows the z-axis, vectors represent the directions $\vec{A}$ and $\vec{B}$, and different shades indicate different measurement settings. θ is the angle between the primary measurement axes of Alice and Bob. We vary θ to test the rotational (in)variance of the three correlation functions.

4. Quantum nonlocality tests

We first derive an entanglement test. For any single qubit state $|\psi\rangle$ with $\mathbb{B} =$ trine,

$$|\langle\vec{B}\rangle| = \left|\sum_{j=1}^{M} \vec{B}_j \langle\psi|\hat{E}_j|\psi\rangle\right| \leqslant \frac{1}{2}. \tag{10}$$

The proof is similar to that for the singlet correlations, equation (9). Thus, if Alice and Bob have a separable state, and both make trine measurements, then

$$|\langle\vec{A}\cdot\vec{B}\rangle| \leqslant \frac{1}{2}\times\frac{1}{2} = \frac{1}{4}. \tag{11}$$

But for the singlet state, using equation (9)

$$|\langle\vec{A}\cdot\vec{B}\rangle| = \frac{1}{2} > \frac{1}{4}. \tag{12}$$

Thus, equation (11) can be violated, and so is a useful witness of entanglement, attaining the minimum $W_{\mathrm{E}} = 9$.

We can derive an EPR-steering inequality [30] in a very similar way, but with Alice using two orthogonal (in the Bloch sphere sense) projective measurements, $\mathbb{A}$ and $\mathbb{A}'$. We thus have,

for any pair of Alice's results,

$$|\vec{A} + \vec{A}'| \leqslant 2\cos\frac{\pi}{4} = \sqrt{2}. \tag{13}$$

Note that this makes no use of quantum mechanics, but is a property only of the vectorial values of the results Alice reports. This is as required for a rigorous demonstration of EPR-steering [3]. But Bob still trusts his apparatus so under the assumption that Bob has a local quantum state unaffected by Alice's choice of setting, equation (10) still applies [3]. Thus for $\mathbb{B}$ = trine we can derive

$$|\langle(\vec{A} + \vec{A}') \cdot \vec{B}\rangle| \leqslant \sqrt{2} \times \frac{1}{2} = \frac{1}{\sqrt{2}}. \tag{14}$$

For a singlet state, however, we have from equation (9),

$$|\langle(\vec{A} + \vec{A}') \cdot \vec{B}\rangle| = 1 > \frac{1}{\sqrt{2}}. \tag{15}$$

Thus, equation (14) is an EPR-steering inequality [30] that can be violated and attains the minimum value of $W_S = 12$.

We note finally that the CHSH inequality

$$|\langle AB + A'B + AB' - A'B'\rangle| \leqslant 2, \tag{16}$$

which achieves the minimum cost of $W_B = 16$, is not of the form that we considered for entanglement and EPR-steering; the variables A, A', B and B' are not unit-vectors but rather take the values ± 1.

5. Experiment

We experimentally demonstrated the maximally parsimonious tests defined above using photonic qubits, employing the polarization encoding $|H\rangle \equiv |0\rangle$ and $|V\rangle \equiv |1\rangle$. The entangled photons are generated from a type-I 'sandwich' bismuth borate spontaneous parametric down conversion source [31]. The entangled state produced is the maximally entangled Bell state $|\Phi^+\rangle = (|00\rangle + |11\rangle)/\sqrt{2}$. We rotate $|\Phi^+\rangle$ to the desired singlet state, $|\Psi^-\rangle = (|01\rangle - |10\rangle)/\sqrt{2}$, using standard polarizing optics; see figure 2 for details. The apparatus can be readily reconfigured to demonstrate each nonlocality test. We also perform quantum state tomography [32], which allows us to determine the quality of the experimentally produced states.

The entangled state we produce has a fidelity of $(97 \pm 1)\%$ with the ideal singlet, allowing us to easily violate all of our inequalities. The slight infidelity is caused by three effects, each making an approximately equal contribution. Imperfect collection of correlated photons produces a small amount of symmetric (depolarization) noise. Imperfect temporal walk-off compensation causes dephasing noise, which is not symmetric. Imperfect compensation of unwanted birefringence leads to a small local unitary rotation of the state, away from the symmetric singlet state. After allowing for the local unitary rotation, our experimental state has a fidelity of 99% with the closest Werner state [2].

Each quantum nonlocality inequality requires different optical elements. To demonstrate Bell nonlocality, by violating a CHSH inequality [17], only projective measurements are needed. Demonstrating maximally parsimonious EPR-steering and entanglement witnesses requires at

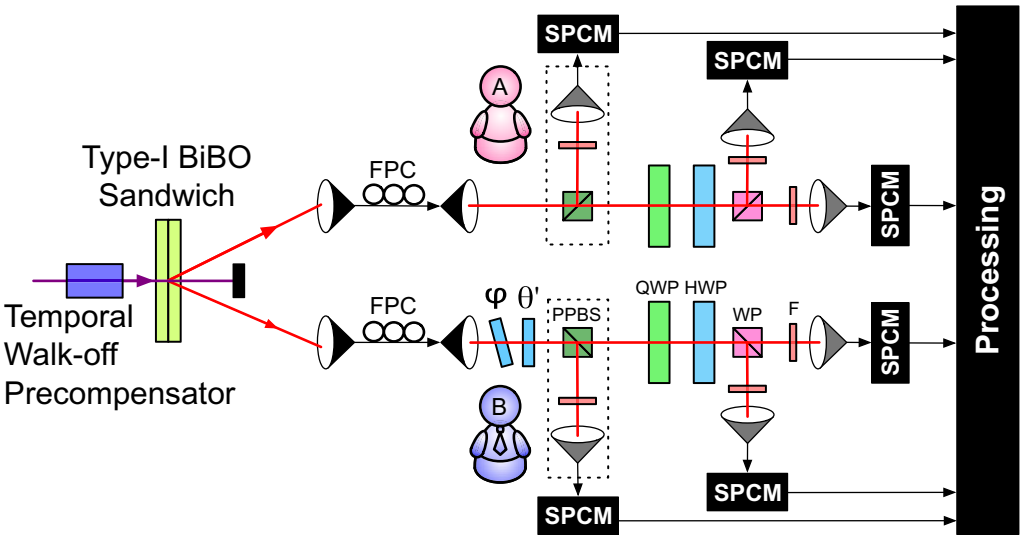

Figure 2. Experimental setup. Alice's laboratory is the top rail, while Bob's is the bottom. A frequency-doubled mode-locked 820 nm Ti-sapphire laser with a 80 MHz repetition rate drives a type-I parametric down converter in the sandwich configuration [31], coupled into single mode fibres (black). Fibre polarization controllers (FPC), combined with a phase shift φ, rotate the entangled state to the desired singlet state. The CHSH measurement schemes shown in figure 1 are implemented using half wave plates (HWP), quarter wave plates (QWP) and polarizing Wollaston prisms (WP). Partially polarizing beam splitters (PPBS) (dotted boxes) are inserted into the beam path when needed to implement the trine measurements. The photons are filtered with 3 nm FWHM filters (F) and then collected via multi mode fibres (grey) onto single photon counting modules (SPCM).

least one nonprojective measurement. We simultaneously monitored all measurement outcomes, whilst calibrating for different channel efficiencies; see figure 2 and appendix for details.

We implement the nonprojective trine measurement using the techniques of [19]. The three POVM elements $\hat{E}_j$ are proportional to projectors onto the following three states, for the case $\theta = 0$ (see figure 1),

$$|T_0\rangle = |1\rangle\,,\ |T_\pm\rangle = -\frac{\sqrt{3}}{2}\,|1\rangle \pm \frac{1}{2}\,|0\rangle\,.$$

Each of these states is separated by an angle of $\frac{2\pi}{3}$ in the x–z plane of the Bloch sphere. The weighting b_j or a_j appearing in each POVM element is $\frac{1}{3}$. To implement such a measurement, a partially projecting polarizing element is added to the set-up to allow us to produce the required projectors with the appropriate weights. Specifically, we employ a partially polarizing beam splitters (PPBS) with transmissivities $\tau_{\rm V} = \sqrt{1/3}$ and $\tau_{\rm H} = 1$, and reflectivities $r_{\rm V} = \sqrt{2/3}$ and $r_{\rm H} = 0$. This allows us to implement the measurement $\langle T_0|$ at the reflecting port of the PPBS. A measurement of σ_x is then performed using a half wave plates (HWP) at $\frac{\pi}{8}$ and a Wollaston prism on the transmitted port; the two outputs represent the outcomes $\langle T_+|$ and $\langle T_-|$. For those cases where a two-outcome projective measurement is required (rather than a trine

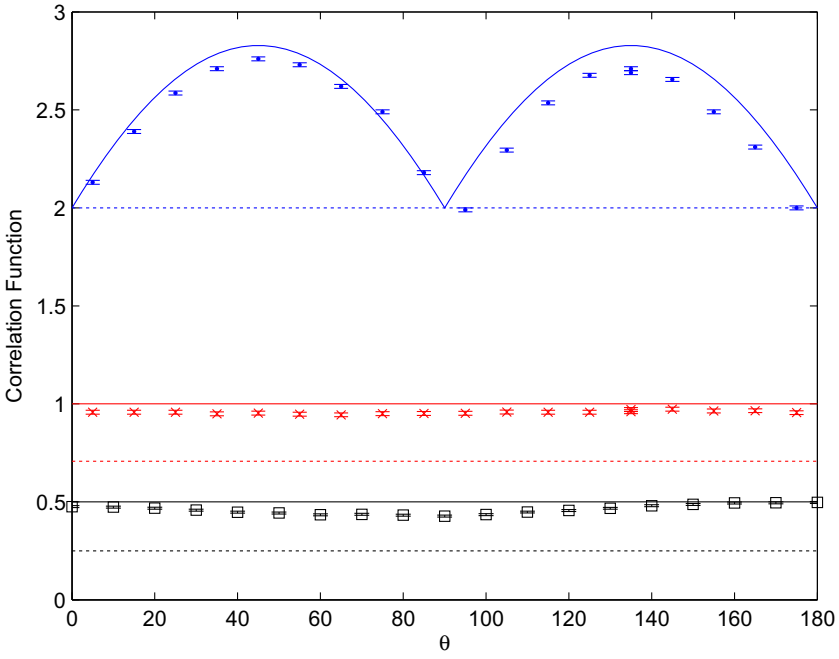

Figure 3. Alignment dependence of nonlocality measures. The top (blue), middle (red) and bottom (black) data and curves show the dependence on θ (figure 1) of the CHSH, EPR-steering and entanglement tests, respectively. Solid lines are the theoretical values for a perfect singlet state, the dashed lines represent the bounds for each nonlocal task and the points are experimentally determined values.

measurement), the PPBS is omitted. In all cases, Bob can rotate the orientation of his measurement setting by the angle θ shown in figure 1 by using the HWP labelled θ' ($\theta'/4 = \theta$) in figure 2.

The results for each correlation function, as θ varies, can be seen in figure 3. The inequality for the CHSH test was varied to take into account the effective relabelling of the measurement outcomes every $\pi/2$. To do this, we replace the right-hand side of equation (16) with $\max(|\mathrm{perm}([-1, 1, 1, 1]) \cdot [AB, A'B, AB', A'B']|)$. This ensures that the CHSH test is violated for almost all values of θ, but the degree of violation depends strongly upon θ. By contrast, the EPR-steering and separability demonstrations are observed to be almost completely rotationally invariant. The systematic deviations from the predicted complete rotational invariance arise predominantly from imperfections in symmetrically implementing the rotated trine measurement. Slightly imperfect splitting ratios (errors of about 1–2%) of the PPBS makes the experimental trine measurement slightly asymmetric. Additionally, the slightly imperfect retardance of the half-wave plate (θ' in figure 2) tilts the trine measurement out of the desired plane in Bloch space in a setting-dependent manner.

In this experiment, we violate the three correlation functions with the maximally entangled singlet state, a Werner state with purity parameter $\eta = 1$ [2]. We do not vary η in our demonstration of the maximally parsimonious tests because each of the correlations would simply be scaled by η for each value of θ. We previously used Werner states to investigate the noise tolerance (minimum value of η required) for each type of quantum nonlocality [8].

6. Conclusion

We have shown that the complexity cost, W, of the nonlocal phenomena of Bell nonlocality, EPR-steering and entanglement form a strict hierarchy ($W_B > W_S > W_E$), reflecting the strength of the concept of nonlocality being tested in each case [3]. We have done this by introducing new inequalities for EPR-steering and entanglement that are the simplest possible *witnesses* for these types of nonlocality. That is, a positive result confirms the effect has been seen. Note, however, that a negative result does not necessarily mean the effect is not present in our experiment, as a different inequality (using the same detector settings) might detect it. Moreover, for particular classes of states it is likely that one could design equally parsimonious tests, using different measurement settings, which would allow demonstrations of EPR-steering and entanglement when our measurement settings do not. None of this alters the key point that no states or measurement settings allow for tests that are more parsimonious than those we have derived and demonstrated.

The tests we introduce for EPR-steering and entanglement could have practical application in entanglement distribution. Because they use the minimum number of joint measurement settings, and the minimum number of joint outcomes, it is possible that our protocols would maximize the rate for performing these tasks. We note, however, that this would depend also on statistical errors and the weights given to the different settings. The fact that the degree of violation is independent of the relative orientation of the two polarizers could have technological advantages in implementations using optical fibres. It is also of theoretical interest, showing the application of the concepts of two-designs to quantum nonlocality.

Acknowledgments

Part of this research was conducted by the Australian Research Council Centre of Excellence for Quantum Computation and Communication Technology (project no. CE110001029). SMB thanks the Royal Society and the Wolfson Foundation for support.

Appendix. Measurement efficiency

The different measurement outcomes have slightly different efficiencies due to small experimental imperfections. These measurement channel imperfections, at the level of a few per cent or less, include unit-to-unit variation in the efficiencies of the single photon counting modules, and slight imbalances in fibre coupling efficiencies. The different efficiencies of the measurement outcomes could lead to errors in the correlation function if not compensated. We fix this problem by carefully measuring the relative efficiencies (i.e. the ratios of measurement channel efficiencies). We post-process the measurement data to reduce the efficiency in high-efficiency channels so that all relative measurement efficiencies are effectively the same.

The ratio of channel efficiency is defined as $\eta_{nm} = \eta_n/\eta_m$, where η is the efficiency after separation on a (P)PBS into output channels n and m. The correction factor η_{nm} can be calculated by measuring both $\hat{\sigma}_x$ and $-\hat{\sigma}_x$, by rotating a waveplate before the splitting device, and comparing the count rates after the eigenvectors switch channels. To apply the correction, we take the raw counts C_n and C_m for a particular setting, then multiply C_m by η_{nm} to correct for any asymmetric loss. This effectively gives both channels the same loss, η_n. This calibration technique allows for a demonstration of the nonlocality tests whilst minimizing the

systematic error from unbalanced channel efficiencies. The observed channel efficiency ratios varied between 0.9 and 1.1 for all combinations of the six different output channels.

References

[1] Bell J S 1964 *Physics* **1** 195–200
[2] Werner R F 1989 *Phys. Rev.* A **40** 4277
[3] Wiseman H M, Jones S J and Doherty A C 2007 *Phys. Rev. Lett.* **98** 140402
[4] Jones S J, Wiseman H M and Doherty A C 2007 *Phys. Rev.* A **76** 052116
[5] Einstein A, Podolsky B and Rosen N 1935 *Phys. Rev.* **47** 777–80
[6] Reid M D, Drummond P D, Bowen W P, Cavalcanti E G, Lam P K, Bachor H A, Andersen U L and Leuchs G 2009 *Rev. Mod. Phys.* **81** 1727–51
[7] Schrödinger E 1935 *Proc. Camb. Phil. Soc.* **31** 555–63
[8] Saunders D J, Jones S J, Wiseman H M and Pryde G J 2010 *Nature Phys.* **6** 845–9
[9] He Q Y, Drummond P D and Reid M D 2011 *Phys. Rev.* A **83** 032120
[10] Acín A, Brunner N, Gisin N, Massar S, Pironio S and Scarani V 2007 *Phys. Rev. Lett.* **98** 230501
[11] Branciard C, Cavalcanti E G, Walborn S P, Scarani V and Wiseman H M 2012 *Phys. Rev.* A **85** 010301
[12] Bennet A J, Evans D A, Saunders D J, Branciard C, Cavalcanti E G, Wiseman H M and Pryde G J 2012 *Phys. Rev.* X **2** 031003
[13] Smith D H *et al* 2012 *Nature Commun.* **3** 625
[14] Wittmann B, Ramelow S, Steinlechner F, Langford N K, Brunner N, Wiseman H M, Ursin R and Zeilinger A 2012 *New J. Phys.* **14** 053030
[15] Toner B F and Bacon D 2003 *Phys. Rev. Lett.* **91** 187904
[16] Montina A 2012 *Phys. Rev. Lett.* **109** 110501
[17] Clauser J F, Horne M A, Shimony A and Holt R A 1969 *Phys. Rev. Lett.* **23** 880–4
[18] Barnett S M 2009 *Quantum Information* (New York: Oxford University Press)
[19] Clarke R B M, Kendon V M, Chefles A, Barnett S M, Riis E and Sasaki M 2001 *Phys. Rev.* A **64** 012303
[20] Bancal J, Brunner N, Gisin N and Liang Y 2011 *Phys. Rev. Lett.* **106** 020405
[21] Martens H and de Muynck W M 1990 *Found. Phys.* **20** 255
Martens H and de Muynck W M 1990 *Found. Phys.* **20** 357
[22] Wiseman H M and Milburn G J 2010 *Quantum Measurement and Control* (Cambridge: Cambridge University Press)
[23] Renes J M, Blume-Kohout R, Scott A J and Caves C M 2004 *J. Math. Phys.* **45** 2171
[24] Ambainis A and Emerson J 2007 *Proc. 22nd Annual IEEE Conf. on Computational Complexity* (*San Diego*) pp 129–40
[25] Dankert C, Cleve R, Emerson J and Livine E 2009 *Phys. Rev.* A **80** 012304
[26] Bendersky A, Pastawski F and Paz J P 2009 *Phys. Rev.* A **80** 032116
[27] Delsarte P, Goethals J M and Seidel J J 1977 *Geom. Dedicata* **6** 363–88
[28] Brunner N and Gisin N 2008 *Phys. Lett.* A **372** 3162–7
[29] Hong Y 1982 *Eur. J. Comb.* **3** 255–8
[30] Cavalcanti E G, Jones S J, Wiseman H M and Reid M D 2009 *Phys. Rev.* A **80** 032112
[31] Altepeter J B, Jeffrey E R and Kwiat P G 2005 *Opt. Express* **13 22** 8951–9
[32] James D F V, Kwiat P G, Munro W J and White A G 2001 *Phys. Rev.* A **64** 052312